J Solid State Electrochem (2001) 5: 479–486
DOI 10.1007/s100080000177

ORIGINAL PAPER

Aigars Vītiņš

Study of the alternating current electrical properties of ZrO_2–7.5 mol% Y_2O_3 ceramics at room temperature and at 457–595 K

Received: 3 May 2000 / Accepted: 4 October 2000 / Published online: 4 July 2001

Abstract The impedance of a ZrO_2–7.5 mol% Y_2O_3 ceramic specimen was measured using the two-probe technique in the frequency range 20 Hz–1 MHz at room temperature and in the temperature range 457–595 K. The novelty of the research lies in the analysis of the intragrain part of the impedance spectra of the ceramics on the basis of the approach proposed in the literature for impedance of ZrO_2–Y_2O_3 single crystals. The method to determine a value of the intragrain direct current electrical conductivity from an impedance spectrum has been developed. The frequency dependence of the intragrain complex dielectric response was interpreted according to the common model used in the literature. Frequency domains, where a power-law dependence having different exponents $n_1 = 0.825$–0.844 and $n_2 = 0.571$–0.592 is observed, were found. The inner consistency of the model used is verified. Values of the transition frequency and the relaxation frequency were determined for the grain interiors and compared with each other. The values of the activation energies of the direct current conductivity, the transition frequency and the relaxation frequency are found to be the same within experimental uncertainty in the temperature range 457–523 K.

Keywords Yttria-stabilized zirconia · Ceramics · Intragrain impedance · Ionic conductivity · Frequency

Presented at the international conference "Solid State Chemistry 2000", 3–8 September 2000, Prague, Czech Republic

A. Vītiņš
Institute of Solid State Physics, University of Latvia,
Ķengaraga ielā 8, LV-1063 Riga, Latvia
E-mail: vitinsa@latnet.lv
Tel.: +371-7187817
Fax: +371-7112583

Introduction

Yttria-stabilized zirconia, ZrO_2–Y_2O_3, is known to be an essentially oxygen-ionic conductor at high temperatures, well above room temperature [1, 2, 3, 4, 5]. Alternating current (a.c.) electrical measurements and the complex impedance or admittance representation allow the separation of several contributions to the total direct current (d.c.) resistance of a ceramic specimen with reversible electrodes, arising from the grain interior and grain boundary resistances and the polarization resistance at the electrode–electrolyte interfaces, whenever the related time constants for the individual processes are sufficiently different [6, 7, 8, 9, 10, 11]. Thus, the electrical properties relevant to crystallites of ceramics can be studied by means of the impedance method [11].

The aim of this study was to analyze the intragrain part of an impedance spectrum of ZrO_2–7.5 mol% Y_2O_3 ceramics at 457–595 K to find a value of the intragrain d.c. electrical conductivity, σ_{DC}, to apply a model for the interpretation of the frequency dependence of the complex dielectric response, $\epsilon_T(\omega) = \epsilon'(\omega) - j\epsilon'(\omega)$, where $j \cdot j = -1$. The intragrain part of an impedance spectrum of ZrO_2–7.5 mol% Y_2O_3 ceramics was interpreted according to the approach proposed by Abelard and Baumard [12] for the impedance arising from the bulk conduction in a ZrO_2–12 mol% Y_2O_3 single-crystal sample. For comparison, the complex dielectric permittivity of the ceramics at room temperature, 291–298 K, is also presented as a function of frequency.

Experimental

The ZrO_2–7.5 mol% Y_2O_3 ceramic specimen with silver electrodes used in this investigation has already been characterized [13]. The ceramic specimen was obtained from ZrO_2–7.5 mol% Y_2O_3 powder having a specific surface area of 30 m^2/g synthesized in air plasma. The ceramic specimen has a density of 95–96% of the theoretical value [13]. The as-prepared ceramics contained a single crystalline phase having a face-centered fluorite-type cubic structure [3, 13, 14].

The impedance spectra were measured using the two-probe technique for the ceramic specimen in air in the frequency range 20 Hz–1 MHz at room temperature, 291–298 K, and in the temperature range 457–595 K by means of a HP 4284A precision LCR meter under the following measurement conditions: the measurement parameters C_p, D at 291–298 K and R, X at 457–595 K, ten frequency measurement points per decade, test signal voltage 1 V root mean square, long integration time, averaging 16. The temperature near the specimen was measured by means of a chromel–alumel thermocouple and a V7-39 voltmeter (Minsk, Belarus). The temperature was maintained constant within 0.25 K during the measurements.

A high-temperature specimen holder with two silver leads each of length 0.44 m was used for the impedance measurements at 457–594 K. Four coaxial cables each of length 1.5 m were connected in the four-terminal-pair configuration and were used to interconnect the leads of the holder and terminals of the HP 4284A precision LCR meter. The residual capacitance of the specimen holder was found to be 0.28 pF. The impedance data measured were corrected taking the residual capacitance into account.

At room temperature, 291–298 K, a simple specimen holder made from textolite with two short silver leads each of length less than 1 cm was used to interconnect the specimen and the terminals of the HP 4284A meter with the HP 16047C test fixture.

Results and Interpretation

Impedance at room temperature

The real $\epsilon'(\omega) = C_p(\omega)/(\epsilon_0 L)$ and imaginary $\epsilon''(\omega) = \epsilon'(\omega)D(\omega)$ parts of the complex dielectric permittivity were obtained as functions of the angular frequency, ω, $\omega = 2\pi\nu$, where ν is the frequency in hertz, from the impedance data of the ZrO_2–7.5 mol% Y_2O_3 ceramic specimen at 291–298 K, $C_p(\omega)$ is the parallel capacitance, $D(\omega)$ is the dissipation factor, ϵ_0 is the electric constant, $\epsilon_0 = 8.854$ pF/m and $L = S/H$, where S is the cross-sectional area and H is the specimen thickness. A small steady decrease of $\epsilon'(\omega)$ by 2% from 26.2 to 25.7 and a decrease of $\epsilon''(\omega)$ from 0.303 to 0.059 were observed as ν increased from 300 Hz to 1 MHz at 292 K (Fig. 1, curve 1) before the measurement series at 457–595 K. The values of $\epsilon'(\omega)$ at 100 kHz and 1 MHz, 25.8 and 25.7, respectively, are in agreement with the value [12] of the high-frequency dielectric permittivity of the samples made from a single crystal $[(ZrO_2)_{0.88}$–$(Y_2O_3)_{0.12}]$, $\epsilon_\infty = 25 \pm 1$ at 100 kHz and room temperature. Increased dispersion of $\epsilon'(\omega)$ and increased dielectric loss, $\epsilon''(\omega)$, were observed after the measurement series at 457–595 K (Fig. 1, curves 3, 4 in comparison with curves 1, 2). A power-law dependence, $\epsilon''(\omega) \propto \omega^{n-1}$, was observed: $n = 0.75$ (Fig. 1b, curves 1, 4), $n = 0.81$ (Fig. 1b, curve 2) in the frequency range 2–12 kHz and $n = 0.66$ (Fig. 1b, curve 3) in the frequency range 4–60 kHz.

Impedance complex plane plots at 457–595 K

A representative example of the impedance complex plane plots, $Z(\omega) = \mathrm{Re}(Z) + j\mathrm{Im}(Z)$, is shown in Fig. 2. The impedance plot can be empirically approximated by

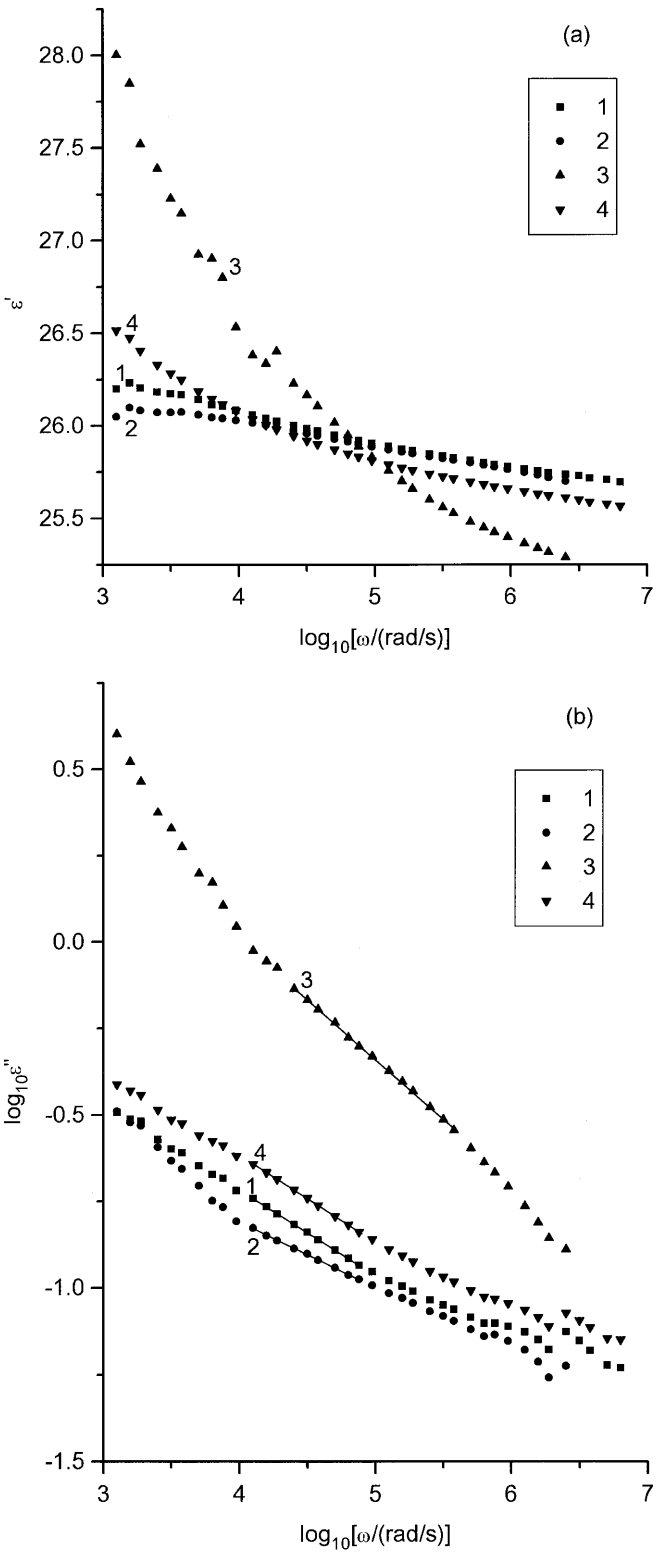

Fig. 1 Plots of **a** the real $\epsilon'(\omega)$ and **b** the imaginary $\epsilon''(\omega)$ parts of the complex dielectric permittivity as functions of the frequency ω for the ZrO_2–7.5 mol% Y_2O_3 ceramic specimen in the sample holder with short leads (*1*, *4*) and in the high-temperature holder (*2*, *3*) at room temperature 292 K (*1*, *2*) and 298 K (*3*, *4*) before (*1*, *2*) and after (*3*, *4*) the measurement series at 457–595 K

a part of a circle passing through the origin [12, 15]. The center of the circle is displaced below the real axis by an angle, θ, of 15.2°. θ was 14.1–15.7° during the heating and cooling cycles of the whole measurement series in the temperature range 457–595 K. The part of the circle corresponds to polarization and intragrain conduction in ceramics according to the literature [7, 8, 9, 10, 11]. The intersection of the circle with the real axis gives the intragrain d.c. resistance, R_{DC}, of the specimen [7]. The low-frequency, 20–40 Hz, data points in Fig. 2 form the beginning of the second impedance arc caused by grain boundary resistance in the ceramics [7, 8, 9, 10, 11, 13].

Two kinds of small systematic deviations of the data points from the part of the empirical circle are present in Fig. 2. High-frequency data points at frequencies well above 2 kHz at 479.7 K are located above the part of the circle (Fig. 2). This deviation is because $\epsilon'(\omega)$ approaches ϵ_∞ at increasing frequencies [12]. Another kind of deviations is at frequencies well below 2 kHz down to 50 Hz at 479.7 K: a local minimum of –Im(Z) (Fig. 2). The systematic deviations of the data points from the empirical circle mean that initially from an impedance plot only an approximate value of R_{DC} can be evaluated at the end of the first impedance arc. The way to find the empirical circle and the value of R_{DC} from the intragrain part of an impedance spectrum is proposed in the following section on the basis of the impedance data analysis in accordance with the literature [12] for yttria-stabilized zirconia single-crystal samples.

Complex dielectric response at 457–595 K

The complex dielectric response, $\epsilon_T(\omega)$, was obtained at 457–595 K by subtracting the d.c. conductivity, σ_{DC}, $\sigma_{DC} = 1/(R_{DC}L)$, from the total conductivity, $\sigma_T(\omega)$, $\sigma_T(\omega) = 1/[Z(\omega)L]$, according to Ref. [12]: $\epsilon_T(\omega) = [\sigma_T(\omega) - \sigma_{DC}]/(j\epsilon_0\omega)$. The value of R_{DC} affects only the imaginary part $\epsilon''(\omega)$, particularly, at low frequencies. Initially $\epsilon''(\omega)$ was calculated from the impedance data taking into account the initial approximate value of R_{DC}.

A log–log plot of $\epsilon'(\omega)$ and $\epsilon''(\omega)$ as a function of the angular frequency, ω, at 479.7 K is shown in Fig. 3. The frequency range of the intragrain conduction and polarization may be subdivided into two domains, below and above the transition frequency, ω_T [12], where a power-law dependence is observed, $\epsilon''(\omega) \propto \omega^{n-1}$, but with different exponents $n_1 = 0.83$ and $n_2 = 0.58$, respectively. A value of R_{DC} was selected in order to parallel the linear parts of the log–log plot of $\epsilon'(\omega)$ and $\epsilon''(\omega)$ as a function of ω below ω_T as shown in Fig. 3. Thus, the frequency dependence of $\epsilon_T(\omega)$ below ω_T is made similar to that for a $[(ZrO_2)_{0.88}$–$(Y_2O_3)_{0.12}]$ single-crystal sample [12] by means of the appropriate selection of the value of R_{DC}. The distance between the parallel straight lines of $\epsilon'(\omega)$ and $\epsilon''(\omega)$ for $\omega < \omega_T$ along the ordinate axis is $\log_{10}[\tan(n_1\pi/2)]$ related to their slope n_1 according to the Kramers–Kronig relations as described in Ref. [12]. Indeed, the distance between $\epsilon'(\omega)$ and $\epsilon''(\omega)$ along the ordinate axis is close to $\log_{10}[\tan(n_1\pi/2)]$, which proves the inner consistency of the applied model with the selected value of R_{DC}. For instance, at 479.7 K of the heating cycle, $\log_{10}[\epsilon''(\omega)/\epsilon'(\omega)] = -0.567$ in the power-law range of frequency $\omega < \omega_T$ and $\log_{10}[\tan(n_1\pi/2)] = -0.563$. The difference between these two quantities was within 2.3% of their values for the impedance spectra of the heating and cooling cycles of the temperature range

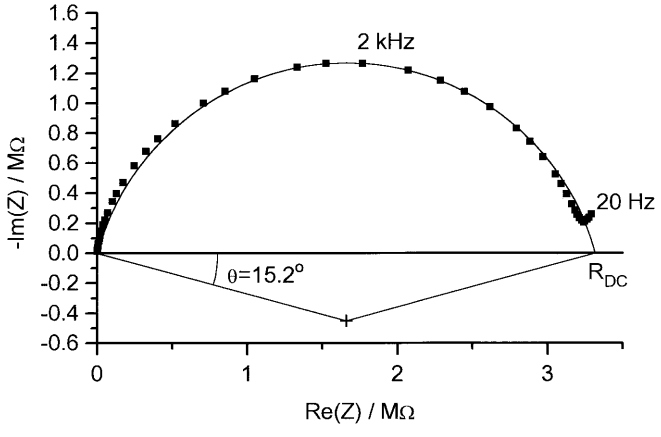

Fig. 2 Impedance plot for the ZrO_2–7.5 mol% Y_2O_3 ceramic specimen at 479.7 K in the heating cycle. The direct current resistance, R_{DC}, is found to be equal to 3.316 MΩ. The circle, whose center is identified with a *cross*, is depressed below the real axis by an angle $\theta = 15.2°$

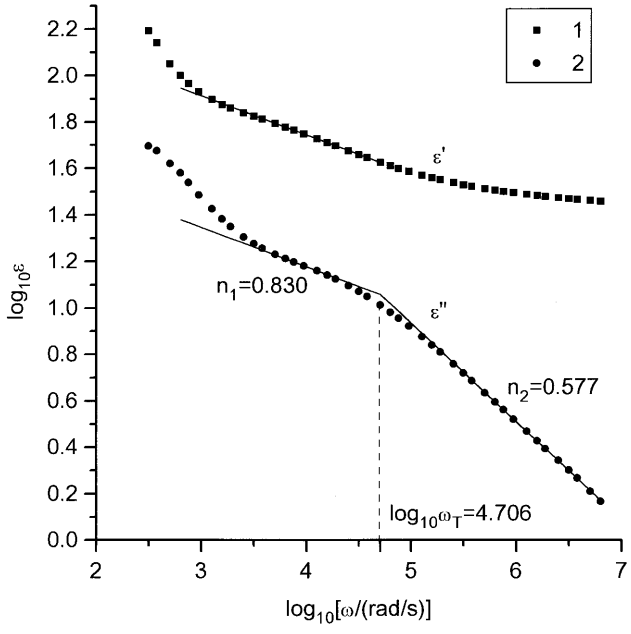

Fig. 3 Log–log plot of the real (*1*) and imaginary (*2*) parts of the complex dielectric response of the ZrO_2–7.5 mol% Y_2O_3 ceramic specimen at 479.7 K as a function of frequency (heating cycle). $R_{DC} = 3.316$ MΩ. The values of the exponents n_1 and n_2 of the power-law dependences are shown. The value of the transition frequency, ω_T, is found in the way as depicted in the plot

457–595 K. Such frequency dependence of $\epsilon_T(\omega)$ corresponds to the constant-phase element (CPE) [15] having the admittance Y_{CPE}:

$$Y_{CPE} = j\omega L\varepsilon_0\varepsilon_T(\omega) = A(j\omega)^{n_1} \quad (1)$$

The CPE connected in parallel with the R_{DC} has the impedance Z_{ZARC}:

$$Z_{ZARC} = \frac{R_{DC}}{1 + R_{DC}A(j\omega)^{n_1}} \quad (2)$$

Z_{ZARC} has an impedance complex plane plot of a depressed circular arc having the depression angle $\theta = (1–n_1)\pi/2$ [15]. The exponents n_1 and n_2 were in the ranges 0.825–0.844 and 0.571–0.592, respectively, at the temperatures 457–595 K both in the heating and in the cooling cycles. n_1 and n_2 were not considerably dependent on temperature.

Temperature dependence of the real dielectric response $\epsilon'(\omega)$

The temperature dependence of the real dielectric response, $\epsilon'(\omega)$, is depicted in Fig. 4 for frequencies, ν, 100 kHz–1 MHz. From room temperature to 470 K, the real dielectric response increases slightly with temperature at frequencies 100 kHz–1 MHz. At temperatures from 470 to 595 K the temperature dependence of $\epsilon'(\omega)$ becomes steeper, particularly for $\nu = 100$ kHz. The frequency dispersion of $\epsilon'(\omega)$ in the ν range 100 kHz–1 MHz increases with increasing temperature.

Intragrain d.c. conductivity

The intragrain d.c. conductivity, $\sigma_{DC} = 1/(R_{DC}L)$, was calculated from values of R_{DC} selected in the way described previously. The temperature dependence σ_{DC} is shown in Fig. 5 as a plot of $\log_{10}(\sigma_{DC}T)$ versus $1000/T$, where T is the absolute temperature. The conductivity is thermally activated. The activation energy is obtained from the slope of the plot. The activation energy is 1.104 ± 0.003 eV in the heating cycle of the whole temperature range studied, 457–595 K, and is 1.094 ± 0.003 eV in the cooling cycle in the range 462–595 K. The deviation of the activation energy value is given in the 95% reliability interval.

Transition frequency

The temperature dependence of the transition frequency, ω_T, is shown in Fig. 6 as a plot of $\log_{10}\omega_T$ versus $1000/T$. ω_T is thermally activated. The activation energy is obtained from the slope of the plot. Values of ω_T were found for the temperature range 457–523 K corresponding to the frequency range investigated (20 Hz–1 MHz). The activation energy values for ω_T are compared with those for σ_{DC} and the relaxation frequency, ω_R, in Table 1. They are found to be equal within experimental uncertainty. ω_R, and the factor K_R are defined in the following subsection.

According to Ref. [12] ω_T can be simply related to the jump frequency of the charge carriers in the solid electrolyte. Yttria dissolved in zirconia substitutes zirconium ions by yttrium ions, Y'_{Zr}, in their lattice sites and forms extrinsic oxygen vacancies, $V_O^{2\cdot}$, the concentration of which is related to the amount of dopant, using the Kröger–Vink notation [12]:

$$Y_2O_3 \rightarrow 2Y'_{Zr} + V_O^{2\cdot} + 3O_O^x \quad (3)$$

ZrO_2–7.5 mol% Y_2O_3, i.e. $Y_{0.14}Zr_{0.86}O_{1.93}$, has a cubic structure of the fluorite type [3, 14], the length of the side of the unit cell being $a = 5.138 \times 10^{-10}$ m [13].

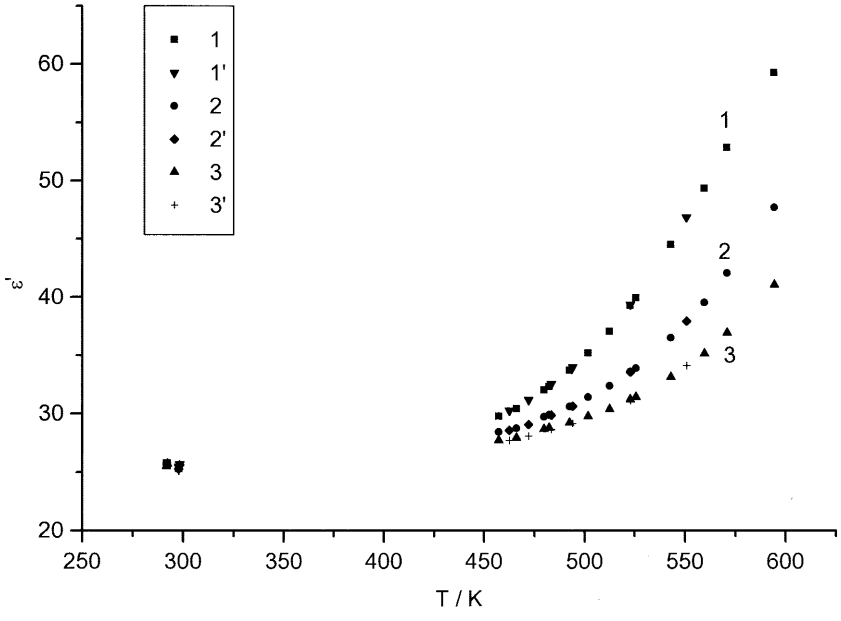

Fig. 4 Plot of the real part of the dielectric response of the ZrO_2–7.5 mol% Y_2O_3 ceramic specimen as a function of temperature for the heating (*1–3*) and cooling (*1′–3′*) cycles at 100 kHz (*1*, *1′*), 400 kHz (*2*, *2′*) and 1 MHz (*3*, *3′*)

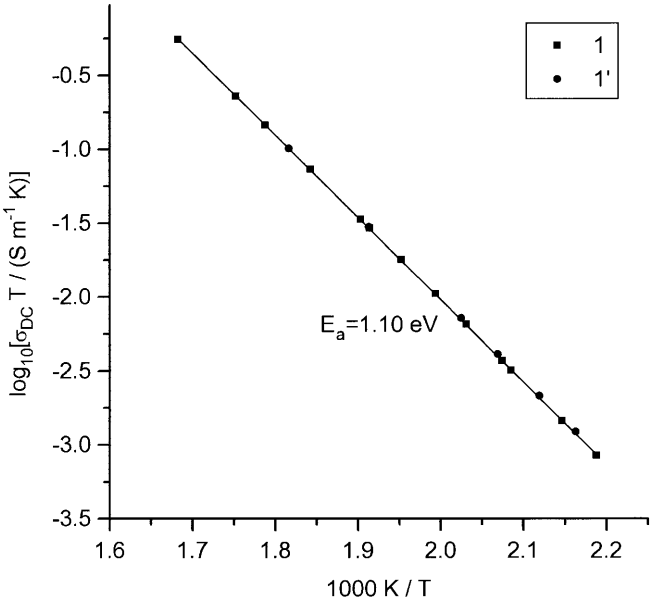

Fig. 5 Plot of the intragrain direct current electrical conductivity, σ_{DC}, of the ZrO_2–7.5 mol% Y_2O_3 ceramic specimen as a function of the temperature, T, in the $\log_{10}(\sigma_{DC}T)$ versus $1000/T$ system of coordinates for the heating (1) and cooling ($1'$) cycles. The value of the activation energy, $E_a = 1.10$ eV, is given in the plot

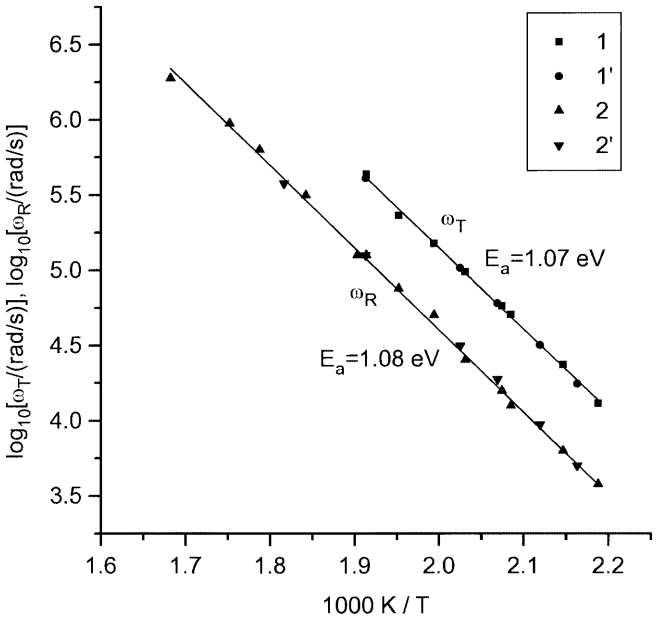

Fig. 6 Plot of the transition frequency ω_T (1, $1'$) and the relaxation frequency ω_R (2, $2'$) as a function of the temperature, T, for the heating (1, 2) and cooling ($1'$, $2'$) cycles. The corresponding values of the activation energies, E_a, are given in the plot

Then, the volume concentration of extrinsic oxygen vacancies, N, is calculated to be

$$N = \frac{4x}{a^3} \tag{4}$$

where x is the number of oxygen vacancies per $Y_{2x}Zr_{1-2x}O_{2-x}$ formula unit. For the ZrO_2–7.5 mol% Y_2O_3 specimen, i.e. $Y_{0.14}Zr_{0.86}O_{1.93}$, $x = 0.07$. The oxygen vacancies are responsible for oxygen-ion conduction in the solid electrolyte. σ_{DC} may be related to the self-diffusion coefficient, D, through the Nernst–Einstein relationship

$$\sigma_{DC} = \frac{DNq^2}{k_B T} \tag{5}$$

where q is the effective charge of the oxygen vacancies and k_B is the Boltzmann constant. For the oxygen vacancies $q = 2e$, where e is the elementary charge. If jumps are assumed to be random and independent of each other, D is related to the mean square displacement of a vacancy after a jump, $\langle r^2 \rangle$, and the mean residence time, $\bar{t}$:

$$D = \frac{\langle r^2 \rangle}{6\bar{t}} \tag{6}$$

Jumps of the oxygen vacancies take place on the primitive cubic oxygen sublattice having the parameter $a/2$. Only jumps to nearest- and next-nearest-neighboring sites are considered [12] along an edge and a face diagonal of a unit cell of the primitive cubic oxygen sublattice, respectively (i.e. along [100] and [110] directions, respectively):

$$\langle r^2 \rangle = \frac{a^2}{4}(1 + p_{110}) \tag{7}$$

where p_{110} is the probability of a jump along the [110] direction, $0 \le p_{110} \le 1$. Combination of Eqs. (4), (5), (6) and (7) yields

$$\nu_T \bar{t} = \frac{e^2 x}{3\pi k_B a} \frac{\omega_T}{\sigma_{DC} T}(1 + p_{110}) \tag{8}$$

where ν_T and ω_T are the transition frequency expressed in hertz and radians per second, respectively, $\omega_T = 2\pi\nu_T$. For the ZrO_2–7.5 mol% Y_2O_3 specimen the numerical value of the first ratio on the right-hand side of Eq. (8), $e^2x/(3\pi k_B a)$, equals 2.688×10^{-8} (S/m)K/(rad/s). $\nu_T\bar{t}$ can be evaluated numerically in accordance with Eq. (8) at given temperatures from the values of σ_{DC} and ω_T obtained as described previously. Then, $\nu_T\bar{t}$ may be expressed as $\nu_T\bar{t} = K_T(1 + p_{110})$, where the values of the factor K_T were found in the ranges given in Table 1. The values of the factor K_T mean that the transition frequency ν_T differs less than 3 times from the inverse of the mean residence time.

Relaxation frequency

The relaxation frequency, ω_R, is defined as the angular frequency of the applied electric field at which the absolute value of the imaginary part of the impedance, $|\mathrm{Im}(Z)|$, has a maximum [10, 11, 16, 17]. The relaxation frequency defines the relaxation time, $t_R = 1/\omega_R$ [17]. The mean time between two consecutive jumps of an oxygen

Table 1 Activation energy values and values of the factors K_T and K_R

Temperature range (K)	Cycle	Activation energy (eV)			K_T	K_R
		σ_{DC}	ω_T	ω_R		
457–523	Heating	1.113 ± 0.004	1.07 ± 0.04	1.11 ± 0.05	0.35–0.43	0.65–0.81
462–523	Cooling	1.098 ± 0.006	1.08 ± 0.03	1.10 ± 0.06	0.37–0.40	0.69–0.77

vacancy is assumed in the literature [16, 17, 18] to be approximately equal to t_R. The temperature dependence of ω_R is shown in Fig. 6 as a plot of $\log_{10}\omega_R$ versus 1000/T. ω_R is thermally activated. The activation energy is obtained from the slope of the plot. The activation energy values for ω_R are given in Table 1. They are found to be equal within experimental uncertainty to the activation energies for σ_{DC} and ω_T. The ratio of ω_T to ω_R was in the range 3.0–4.1 for the intragrain impedance of the ZrO_2–7.5 mol% Y_2O_3 ceramics at a given temperature. ω_R can be compared with the inverse of the mean residence time of an oxygen vacancy in a similar way as v_T in the previous section by means of a combination of Eqs. (4), (5), (6) and (7):

$$\omega_R \bar{t} = \frac{2e^2x}{3k_B a}\frac{\omega_R}{\sigma_{DC}T}(1 + p_{110}) \quad (9)$$

The right-hand side of Eq. (9) may be expressed as $\omega_R\bar{t} = K_R(1 + p_{110})$, where the values of K_R were found in the ranges given in Table 1. In the whole temperature range studied, 457–595 K, the values of K_R were found in the range 0.58–0.81.

Discussion

Comparison of the complex dielectric response at 291–298 and 457–595 K

The values of the real part $\epsilon'(\omega)$ are in the range 25–28 at 291–298 K and correspond to $\log_{10}\epsilon'$ in the range 1.40–1.45. That means a very weak frequency dependence of $\epsilon'(\omega)$ at 291–298 K in comparison to that at 457–595 K. $\epsilon'(\omega)$ increases with temperature. Greater increases of $\epsilon'(\omega)$ are at lower frequencies. However, values of $\log_{10}\epsilon''$ increase considerably more than $\log_{10}\epsilon'$ at temperature increases from 291–298 to 457–595 K.

The power-law dependence of the imaginary part $\epsilon''(\omega)$, $\epsilon''(\omega) \propto \omega^{n-1}$, at room temperature, where n is in the range 0.66–0.81, corresponds to values of $\epsilon'(\omega)$ related to $\epsilon''(\omega)$ as $\epsilon'/\epsilon' = \tan(n_1\pi/2)$. However, the distance at a given frequency between the $\epsilon'(\omega)$ and $\epsilon'(\omega)$ curves in the log–log plot is much greater at room temperature than the distance required by the power-law dependence: for $n = 0.66$–0.81 $\log_{10}(\epsilon'/\epsilon'') = 0.23$–$0.51$. According to the model proposed by Jonscher [19] the $\epsilon'(\omega)$ and $\epsilon''(\omega)$ curves at room temperature may be explained as the fast nonactivated polarization is predominant. In contrast, at low frequencies, ω, below ω_T in the temperature range 457–595 K where $\epsilon'(\omega)$ and $\epsilon''(\omega)$ are related by the power-law dependence, the polarization can be attributed [19] predominantly to thermally activated hopping of charge carriers – possibly oxygen vacancies in ZrO_2–Y_2O_3. Thus, ω_T as the frequency corresponding to the change of the polarization charge carriers contributing mainly to the real part can be explained according to the model [19].

Appreciable differences in the frequency dependences of the complex dielectric permittivity at room temperature (Fig. 1) before and after the measurement series at 457–595 K indicate that the electrical properties of the system studied also depend on its previous thermal state. A period of 20 days elapsed after the furnace had been switched off and had cooled before the final impedance measurements (Fig. 1, curves 3, 4) at room temperature were made. Phenomena of this kind were reported previously [13]. They may be denoted as the "memory" effect [20]. Nevertheless, no significant differences were observed between the data obtained from impedance spectra of heating and cooling cycles in the temperature range 457–595 K (Table 1, Figs. 4, 5, 6), which confirms the thermal stability of the system studied and the reproducibility of the results obtained in the measurement series at 457–595 K.

Comparison of the intragrain part of an impedance spectrum for ceramics with the literature data for single crystals

Because the time constants for the intragrain and grain boundary relaxation are sufficiently different for ZrO_2–Y_2O_3 ceramics [6, 7, 8, 9, 10, 11, 13], it is possible to obtain a part of an impedance spectrum characteristic to the intragrain ZrO_2–Y_2O_3 electrical properties. The intragrain electrical properties are determined by the crystalline part of ceramics; therefore, they may be compared with the electrical properties of single crystals.

One different feature in the frequency dependence of the imaginary part $\epsilon''(\omega)$ for the intragrain part of an impedance spectrum (Fig. 3) is a narrower frequency range of the power-law dependence of $\epsilon''(\omega)$, $\epsilon''(\omega) \propto \omega^{n-1}$, for $\omega < \omega_T$, in comparison with the single crystal studied in Ref. [12]. For ZrO_2–7.5 mol% Y_2O_3 ceramics the frequency range of the power-law dependence for $\omega < \omega_T$ is approximately 0.2–0.3 units of the $\log_{10}\omega$ scale, whereas for a $[(ZrO_2)_{0.88}$–$(Y_2O_3)_{0.12}]$ single crystal this frequency range is approximately one unit of the $\log_{10}\omega$ scale [12].

Both $\epsilon'(\omega)$ and $\epsilon''(\omega)$ deviate towards values higher than those for the power-law dependence at low frequencies $\omega < \omega_T$ (Fig. 3). The deviation in the $\epsilon''(\omega)$ plot starts at higher frequencies, $\log_{10}\omega < 3.5$, than that for $\epsilon'(\omega)$, $\log_{10}\omega < 3$, (Fig. 3). These deviations of $\epsilon'(\omega)$ and $\epsilon''(\omega)$ from the power-law dependence can be attributed to an effect of grain boundary polarization at low frequencies. The low-frequency deviation of the data points below the depressed circular arc (Fig. 2) corresponds to the low-frequency deviation of $\epsilon''(\omega)$ above the power-law dependence for $\omega < \omega_T$ (Fig. 3).

The parameters of the intragrain impedance spectra for the ZrO_2–7.5 mol% Y_2O_3 ceramics both in the heating and in the cooling cycles of the measurement series are compared with those for single crystals in Table 2. No considerable differences are found in the values of the depression angle θ and the exponents n_1 and n_2 for ZrO_2–Y_2O_3 samples having different yttria content, and obtained and studied by different authors.

The characteristic frequencies for ionic conduction

The inverse of the mean residence time of an oxygen vacancy is characterized in the literature as the transition frequency ν_T [12] and the relaxation frequency ω_R [16, 17, 18]. Comparison of the frequencies ν_T and ω_R with the inverse of the mean residence time gives $0.35 \leq \nu_T\bar{t} \leq 0.8$ and $0.58 \leq \omega_R\bar{t} \leq 1.62$ according to Eqs. (8) and (9), respectively, for the probability $0 \leq p_{110} \leq 1$. Thus, ν_T and ω_R are comparable with the inverse of the mean residence time of an oxygen vacancy calculated from Eqs. (4), (5), (6) and (7). The values of K_T found for crystallites of the ZrO_2–7.5 mol% Y_2O_3 ceramics are less than the value of K_T for a $[(ZrO_2)_{0.88}$–$(Y_2O_3)_{0.12}]$ single crystal [12] (Table 2). The values of K_R at 563 K calculated from the data given in Ref. [21] are included in Table 2. They are less than the value of K_R for grain interiors of the ZrO_2–7.5 mol% Y_2O_3 ceramics studied here.

The activation energies for ω_T and ω_R are also found to be equal within experimental uncertainty to the activation energy for σ_{DC} for ZrO_2–Y_2O_3 given in the literature [12, 16, 21] (Table 2). On the other hand, a slightly lower activation energy for ω_R than for σ_{DC} was reported in Ref. [11] for the grain interior impedance semicircle of ZrO_2–12 mol% Y_2O_3 ceramics (Table 2).

Conclusions

1. The impedance plane plots and the frequency dependence of the complex dielectric response of the grain interiors of ZrO_2–7.5 mol% Y_2O_3 ceramics at 457–595 K were interpreted on the basis of the approach proposed in the literature [12] for the ZrO_2–12 mol% Y_2O_3 single crystal. The applicability of a power-law dependence to the intragrain impedance of the ZrO_2–7.5 mol% Y_2O_3 ceramics was evaluated. The method to determine a value of the intragrain σ_{DC} from an impedance spectrum was developed for ceramics. The inner consistency of the model used was verified.
2. The values of ω_T and ω_R for the intragrain impedance of ZrO_2–7.5 mol% Y_2O_3 ceramics were determined in the temperature ranges 457–523 and 457–595 K, respectively. Their ratio at a given temperature was in the range 3.0–4.1.
3. According to the model [19] the fast, nonactivated polarization is predominant in ZrO_2–7.5 mol% Y_2O_3 at room temperature. In contrast, the thermally activated hopping of charge carriers, possibly oxygen vacancies, can be assumed to be the predominant polarization at frequencies ω below ω_T in the temperature range 457–595 K.
4. ν_T and ω_R are comparable with the inverse of the mean residence time of an oxygen vacancy obtained from the Nernst–Einstein relationship assuming jumps of oxygen vacancies to be random and independent of each other.
5. The values of the activation energies for σ_{DC}, ω_T and ω_R are found to be equal within experimental uncertainty in the temperature range 457–523 K.

Table 2 Comparison of parameters for ZrO_2–Y_2O_3 impedance spectra. *g.i.* represents the grain interior part of a spectrum for ceramics and *s.c.* represents a single-crystal sample

Y_2O_3 content (mol%)	Sample	Activation energy (eV)			Depression angle θ	Exponent n_1	Exponent n_2	K_T	K_R	Reference
		σ_{DC}	ω_T	ω_R						
7.5	g.i.	1.10–1.11	1.07–1.08	1.10–1.11	14.1–15.7°	0.825–0.844	0.571–0.592	0.35–0.43	0.58–0.81	This work
6.15	g.i.	1.11	–	1.11	–	–	–	–	0.47[a]	[21]
7	g.i.	1.12	–	1.12	–	–	–	–	–	[16]
8.27	g.i.	1.15	–	1.15	–	–	–	–	0.50[a]	[21]
9.4	s.c.	1.16	–	–	~ 11°	–	–	–	–	[22]
12	s.c.	1.33	1.29	–	14°	0.85	0.64	0.6	–	[12]
12	g.i.	1.224 ± 0.011	–	1.100 ± 0.047	10–12°	–	–	–	–	[11]

[a]At 563 K

Acknowledgements This work was supported financially by grant no. 96.0676 from the Latvian Council of Science.

References

1. Etsell TH, Flengas SN (1970) Chem Rev 70:339
2. Weppner W (1977) Electrochim Acta 22:721
3. Park J-H, Blumenthal RN (1989) J Electrochem Soc 136:2867
4. Beresnev SM (1990) Elektrokhimiya 26:1434 (in Russian)
5. Weppner W (1997) In: Gellings PJ, Bouwmeester HJM (ed) The CRC handbook of solid state electrochemistry. CRC, Boca Raton, pp 295–327
6. Bauerle JE (1969) J Phys Chem Solids 30:2657
7. Verkerk MJ, Middelhuis BJ, Burggraaf AJ (1982) Solid State Ionics 6:159
8. Bentzen JJ, Andersen NH, Poulsen FW, Sørensen OT, Schram R (1988) Solid State Ionics 28–30:550
9. Ciacchi FT, Crane KM, Badwal SPS (1994) Solid State Ionics 73:49
10. Gödickemeier M, Michel B, Orliukas A, Bohac P, Sasaki K, Gauckler L, Heinrich H, Schwander P, Kostorz G, Hofmann H, Frei O (1994) J Mater Res 9:1228
11. Luo J, Hairetdinov EF, Almond DP, Stevens R (1999) Solid State Ionics 122:205
12. Abelard P, Baumard JF (1982) Phys Rev B 26:1005
13. Vītiņš A, Vītiņš Ģ, Krastiņš J, Šteins I, Zālīte I, Lūsis A (1998) J Solid State Electrochem 2:299
14. Yashima M, Kakihana M, Yoshimura M (1996) Solid State Ionics 86–88:1131
15. Macdonald JR (ed) (1987) Impedance spectroscopy emphasizing solid materials and systems. Wiley, New York
16. Orliukas A, Kežionis A, Paulavicius K, Gauckler LJ, Sasaki K, Bohac P (1994) Solid State Phenom 39–40:223
17. Kežionis A, Bogusz W, Krok F, Dygas J, Orliukas A, Abrahams I, Gebicki W (1999) Solid State Ionics 119:145
18. Orliukas A, Bohac P, Sasaki K, Gauckler LJ (1993) In: Poulsen FW, Bentzen JJ, Jacobsen T, Skou E, Østergård MJL (ed) High temperature electrochemical behaviour of fast ion and mixed conductors. Proceedings of the 14th Risø International Symposium on Materials Science. Risø National Laboratory, Roskilde, Denmark, pp 369–374
19. Jonscher AK (1974) Nature 250:191
20. Stoinov ZB, Grafov BM, Savova-Stoinova B, Elkin VV (1991) Electrochemical impedance. Nauka, Moscow (in Russian)
21. Orliukas A, Sasaki K, Bohac P, Gauckler LJ (1991) In: Grosz F, Zegers P, Singhal SC, Yamamoto O (ed) Solid oxide fuel cells. Proceedings of the 2nd International Symposium – Athens, Greece. Commission of the European Communities. – New ways to save energy. Report EUR 13546 EN, pp 377–385
22. de Dios Solier J, Pérez-Jubindo MA, Dominguez-Rodriguez A, Heuer AH (1989) J Am Ceram Soc 72:1500